Sustainable Carbonaceous Biofiller from Miscanthus: Size Reduction, Characterization, and Potential Bio-composites Applications

Tao Wang,[a] Arturo Rodriguez-Uribe,[a] Manjusri Misra,[a,b] and Amar K. Mohanty*,[a,b]

The use of biocarbon derived from renewable resources to substitute for petroleum-based carbonaceous materials in composites and other applications often requires size reduction. Biocarbon obtained by the pyrolysis of miscanthus was subjected to ball milling from 2 to 24 h. Particle analysis was performed by combining scanning electron microscope imaging and image-based particle counting. The milled biocarbon had a highly heterogeneous shape and size distribution, making image-based analysis the most suitable method. The average particle size was reduced from above 3 µm after 2 h of milling to below 1 µm after 24 h of milling. The specific surface area doubled from 148 m²/g to approximately 300 m²/g after 2 h of milling, but it did not change with longer milling. Ball milling caused a gradual decrease of the thermal conductivity from 0.137 to 0.116 $W \cdot m^{-1} \cdot K^{-1}$. The ash content increased from 8 to 17% after 24 h of milling. Polypropylene composites filled with the biocarbon with and without ball milling showed lower density and comparable mechanical properties to a talc-filled composite except for lower impact strength. Using ball milled biocarbon led to a steady increase of the impact strength with longer milling time, reaching values on a par with that of the talc composite.

Keywords: Carbon; Biocarbon; Nano-particles; Milling; Sizing; Composite; Additives

*Contact information: a: Bioproducts Discovery and Development Centre, Department of Plant Agriculture, University of Guelph, Guelph, Ontario N1G 2W1, Canada; b: School of Engineering, University of Guelph, Guelph, Ontario N1G 2W1, Canada; *Corresponding author: mohanty@uoguelph.ca*

INTRODUCTION

Particulate carbon is extensively used in many commercial products including ink, rubber products, automotive parts, coatings, pigments, sensors, catalysts, and energy storage and conversion devices. Most particulate carbon materials, including carbon black, are produced by the incomplete combustion of heavy oil products such as tar. Due to the unsustainable nature of these materials, there have been increased research efforts in using carbon derived from renewable resources in applications such as carbon sequestration, and even in areas traditionally dominated by petroleum-based carbon (Peterson 2012; Aller 2016; Behazin *et al.* 2016). Biochar is the solid fraction obtained after biomass pyrolysis, which produces bio-oil and syngas as the liquid and gas products (Arnold *et al.* 2018). Biochar is rich in carbon, highly porous, and is traditionally used as a natural and low-cost soil amendment material (Amin *et al.* 2016).

Unlike petroleum-based carbonaceous materials that are generated from a highly viscous liquid raw material, biochar derived from biomass can retain some of the tissue and cell structures of the original plant. Reducing biochar to particulate biocarbon is essential for promoting this material as a substitute for conventional carbon products.

Techniques that have been explored for reducing the size of biocarbon include ball milling and vibratory pulverizing (Abdullah and Wu 2009; Peterson *et al.* 2012, 2016). It has been reported that pyrolyzed biomass has much better grindability than the original biomass (Abdullah and Wu 2009). In the same study, the biocarbon was milled to the maximum of 4 min and the particle size was still of a few hundred micrometers.

The particle size along with the size distribution of a particulate material can have strong correlations with its physical and chemical properties, thus having a direct impact on its application and performances. A large number of methods have been developed to study particle sizes and size distributions. These methods can be roughly divided into three groups: separation methods (*e.g.*, the simple sieving method and various sedimentation methods), counting methods (*e.g.*, image analysis and time-of-flight counter), and beam methods (*e.g.*, laser/light diffraction and scattering, focused-beam reflectance, and ultrasonic attenuation spectroscopy) (Naito *et al.* 1998; Li *et al.* 2005).

When the size of the particles of concern is in micrometers and nanometers, the most commonly used methods have been image-based analysis and laser diffraction and scattering. Laser diffraction and scattering is a very popular sizing technique used in research and industry labs due to its fast analysis speed and ease of use. Newer instruments can measure not only solid particles suspended in a liquid medium but also dry powdery material directly. However, based on the principles of the analysis, laser diffraction and scattering method can only provide a reliable measurement of the particle size distribution when the particles are perfect spheres.

Blott and Pye studied the sizes of Ballotini glass beads and sand particles a few hundred micrometers in size using a laser-based technique, and compared the results to those obtained by sieving (Blott and Pye 2006). The laser-based analysis and sieving method produced the same results for the spherical glass beads, but gave very different values for the sand particles with a non-uniform particle shape.

While sieving in the example above is a separation method and can only give size ranges, Califice *et al.* (2013) analyzed particles with different shapes using 2D and 3D images and compared the results to those of laser-based analysis. By using 3D images as the most truthful representation of the particle geometry and size, they found that laser diffraction results present large errors when being used to analyze not only non-spherical particles but also mixtures of particles with different shape populations. Furthermore, besides the shape factor, the parameters entered for the laser diffraction and scattering, in particular the refractive index, can affect the results significantly (Beekman *et al.* 2005).

Image analysis is a counting method, meaning that the particles are inspected one at a time, and the results are the number-based average and distributions. For fine particles, microscopy combined with image analysis can fully reflect particle size, shape, and geometry. The disadvantage is that a sufficient number of particles need to be analyzed to have a comprehensive survey of a sample. This number can be very large, especially in the case of a wide particle size distribution. Image analysis software is often required. As shown later in this study, the morphology of biocarbon is highly heterogeneous, making image-based analysis the most suitable method of choice for sizing the material.

In the present work, biocarbon was produced from miscanthus by pyrolysis and then subjected to size reduction by ball milling. Scanning electron microscopy (SEM) and image analysis were combined to investigate the morphology and sizes of the biocarbon obtained with different ball milling time ranging from 2 h to 24 h. The size and shape changes were then correlated with the changes in the specific surface area, total pore volume, ash content, and thermal conductivity. Finally, in order to evaluate the

performance of the biocarbon as a filler, biocarbon-filled polypropylene composites were fabricated, characterized, and compared to their talc-filled counterparts.

EXPERIMENTAL

Materials

The raw material used was miscanthus harvested in southern Ontario, Canada. The 1 to 3 cm chopped miscanthus containing 10% moisture was pyrolyzed in an oxygen-deprived environment in a continuous pyrolyzer (Metamag Inc., London, ON, Canada) with a built-in screw conveyor at 600 to 650 °C for 10 to 20 min until completely charred. The biochar obtained was ground in a hammer mill to pass a 1/64 in (0.4 mm) screen. Ball milling of the ground biochar was performed by using a Patterson Industries D-Type Ball Mill (Toronto, ON, Canada). The mill contained a ceramic-lined 60-ft long and 72-ft diameter vessel that was filled with 6,000 lbs of ceramic balls with diameters ranging from ¾ to 1½ in, and was operated at a rotational speed of 300 rpm. The pyrolyzed miscanthus biocarbon was milled for 2, 4, 12, 18, and 24 h, and subsequently labeled BcBM2h, BcBM4h, BcBM12h, BcBM18h, and BcBM24h, respectively.

For the preparation of the composites, homopolymer polypropylene, Grade 1120H from Pinnacle Polymers (Garyville, LA, USA), and Fusabond® 353P coupling agent from DuPont Company (Wilmington, DE, USA) were used as the matrix. The talc used in the comparison study was JetFil® P500 talc obtained from Imerys (Oakville, ON, Canada).

Methods

Particle morphology and size analysis

The particles were observed using a Phenom ProX scanning electron microscope of Phenom-World B.V. (Eindhoven, The Netherlands). The sample powder was deposited on carbon tabs adhered to aluminum stubs and imaged without coating. A series of images were taken at different magnifications to capture particles of different sizes. The images were then analyzed using the ParticleMetric particle size analysis application (version 1.0.346.44124) of Phenom-World B.V. to gather the shape and size data of the particles in each image. Because the particles did not have defined geometry, the circle equivalent diameter was used to represent the average size of the particles. Image taking and particle counting were continued until the number average particle size stopped changing noticeably with new additions of images/particles, which indicated that the average size of the particles counted was approaching the true average of the particles in the whole sample. The number of particles measured for each sample was typically more than 3,000.

Specific surface area and pore volume

The surface area and pore volume analysis of the particles was conducted based on the Brunauer–Emmett–Teller (BET) theory, by collecting the adsorption–desorption isotherms of nitrogen at 77 K using an Autosorb-iQ Gas Sorption System by Quantachrome Instruments (Boynton Beach, FL, USA). Each sample was vacuum outgassed overnight before being tested.

Ash content

The ash content was measured by using two different methods. In the first method, the ash was the residue left after the sample was heated in a furnace to constant weight at

750 °C, according to *ASTM D1762 - 84(2013) Standard Test Method for Chemical Analysis of Wood Charcoal*.

In the second method, the heating and weight measurement was taken using a thermogravimetric analyzer (TGA Q500, TA Instruments, New Castle, DE, USA). Approximately 10 mg of a sample was loaded, and the temperature was ramped at 20 °C/min under air purge to 900 °C and held at that temperature for 20 min. The temperature was increased to 1000 °C in the end, and the residual weight was taken as the weight of the ash.

Thermal conductivity and diffusivity

A Hot Disk TPS 500 Thermal Constants Analyzer from ThermoTest Inc. (Fredericton, NB, Canada) was used for the measurement. The sample powder was oven-dried at 105 °C until it reached a constant weight and cooled down to room temperature in a desiccator before being used for testing. The powder was loaded into the cylindrical cavity of the sample holder with a Kapton sensor (Dia: 6.378 mm) inserted in the middle of the powder mass.

Three replicate measurements were taken for each sample, at 120 mW heating power and 60 Hz frequency.

Composites processing and characterization

All fillers were dried to constant moisture content before extrusion. The composites were produced by extrusion and injection molding using a 15-cc micro compounder from Xplore Instruments B.V. (Sittard, The Netherlands). The extruder has three independently controlled heating zones and twin screws with a length of 150 mm and aspect ratio of 18. Compounding was done with a screw speed of 100 rpm, processing temperature of 185 °C in all heating zones, and residence time of 2 min. The samples were molded at 30 °C with an average injection pressure of 10 bar and holding time of 24 sec.

All composites contained 27% filler, 3% coupling agent (Fusabond® P353), and 70% PP (1120H) by weight. Four biocarbon composites were prepared using the biocarbon before ball milling and the materials ball milled for 2, 4, and 24 h (BcBM2h, BcBM4h, and BcBM24h). A talc composite with the same matrix and composition was made using the JetFil® P500 talc. The tensile and flexural properties of the composites were tested using a universal testing machine (UTS-3382 by Instron, Norwood, MA, USA). Tensile tests were conducted using Type IV specimens according to ASTM D638 at a crosshead speed of 5 mm/min.

Flexural properties were tested according to ASTM D790 with a crosshead speed of 14 mm/min and span distance of 52 mm. The Standard Test Method for Unnotched Cantilever Beam Impact Resistance of Plastics ASTM-Designation: D4812 was used for the Charpy impact resistance measurements. The Standard Test Method for Determining the Izod Pendulum Impact Resistance of Plastics ASTM-Designation: D256 was used for the notched Izod tests. The density was measured by using a MDS-300 densimeter by Qualitest (Lauderdale, FL, USA).

The morphology of the composites and the neat polypropylene was studied by imaging the fracture surfaces using the Phenom ProX scanning electron microscope. The sample bars were abruptly fractured in liquid nitrogen and observed without coating. Images were taken at an accelerating voltage of 10 kV.

RESULTS AND DISCUSSION

Particle Size Analysis

The pyrolysis of the miscanthus resulted in black colored char with no considerable size changes from the raw material. The char was hammer milled to pass a 1/64 in (0.4 mm) screen and then ball milled for different lengths of time to yield powders.

As shown in Fig. 1(a), the hammer-milled sample contained large chunky pieces, some of which still clearly represented the cell wall structure of the original biomass. The other images in Fig. 1 showed that ball milling noticeably reduced the particle size.

A number of observations can be made of the ball-milled samples. The sample ball milled for 2 h showed much smaller particle size compared to the hammer-milled sample. However, it still contained a large number of plate-like structures, which appeared to be broken pieces of the original cell wall. The number of these plate-like pieces was much reduced in the 4 h ball-milled sample and difficult to find in the samples milled for longer periods of time. Particles measuring more than one μm could be found in all the samples. Even after extensive ball milling (*e.g.*, 18 h and 24 h), the sizes of these large particles were still comparable to that of the similar particles found in samples milled for shorter periods of time.

However, the images also showed that the particle assemblies grew more "crowded", largely due to the increased presence of the small "dots". Higher magnification images revealed that these dots were sub-micron particles and they tended to aggregate to form a cluster or to decorate the surface of larger particles (Fig. 1 d', e', and f'). All ball-milled samples contained sub-micron particles and the number of sub-micron particles increased with ball milling time. Furthermore, although most of the particles had irregular shape, the particles milled for a longer period of time were less likely to have sharp corners, *i.e.*, they became more spherical.

Because the particles had an irregular shape, image-based analysis was the only reliable method to study their sizes. The sample before ball milling contained very large particles, as shown in Fig. 1(a), making it unsuitable to be sized using an electron microscope. In fact, the ParticleMetric application used in this study has an analysis range of 100 nm to 0.1 mm. Therefore, the size analysis was only performed for the ball-milled samples. Figure 2 shows an example of one image being analyzed. The colored picture on the right demonstrates the "particles" that were recognized. Although not all particles in each image are being recorded, and some overlapping can occur to a small number of particles, the effect becomes negligible when a large number of particles (typically above 3,000 in this study) are measured. The circle equivalent diameter, which is the diameter of a circle that would have the same area as a particle on an image, was used to represent the *size* of the particle.

The average sizes in Fig. 3 confirmed the size reduction with milling time. The average particle size was reduced from 3.2 μm after 2 h of ball milling to 1.1 μm after 18 h of milling and 0.9 μm after 24 h of milling. It is worth pointing out that if one uses the images in Fig. 1 to *manually* measure the particle sizes, one would likely obtain a higher number than the average calculated here because the larger particles can be more conveniently measured. Furthermore, as discussed earlier, image-based analysis is a counting method, and the average calculated is a number average.

The small particles, although less visible, were in much greater numbers than the larger particles. If these samples were analyzed using the laser diffraction and scattering method, one would expect a higher average size because the laser method calculates the

volume average and even a large number of very small particles do not contribute to the volume noticeably.

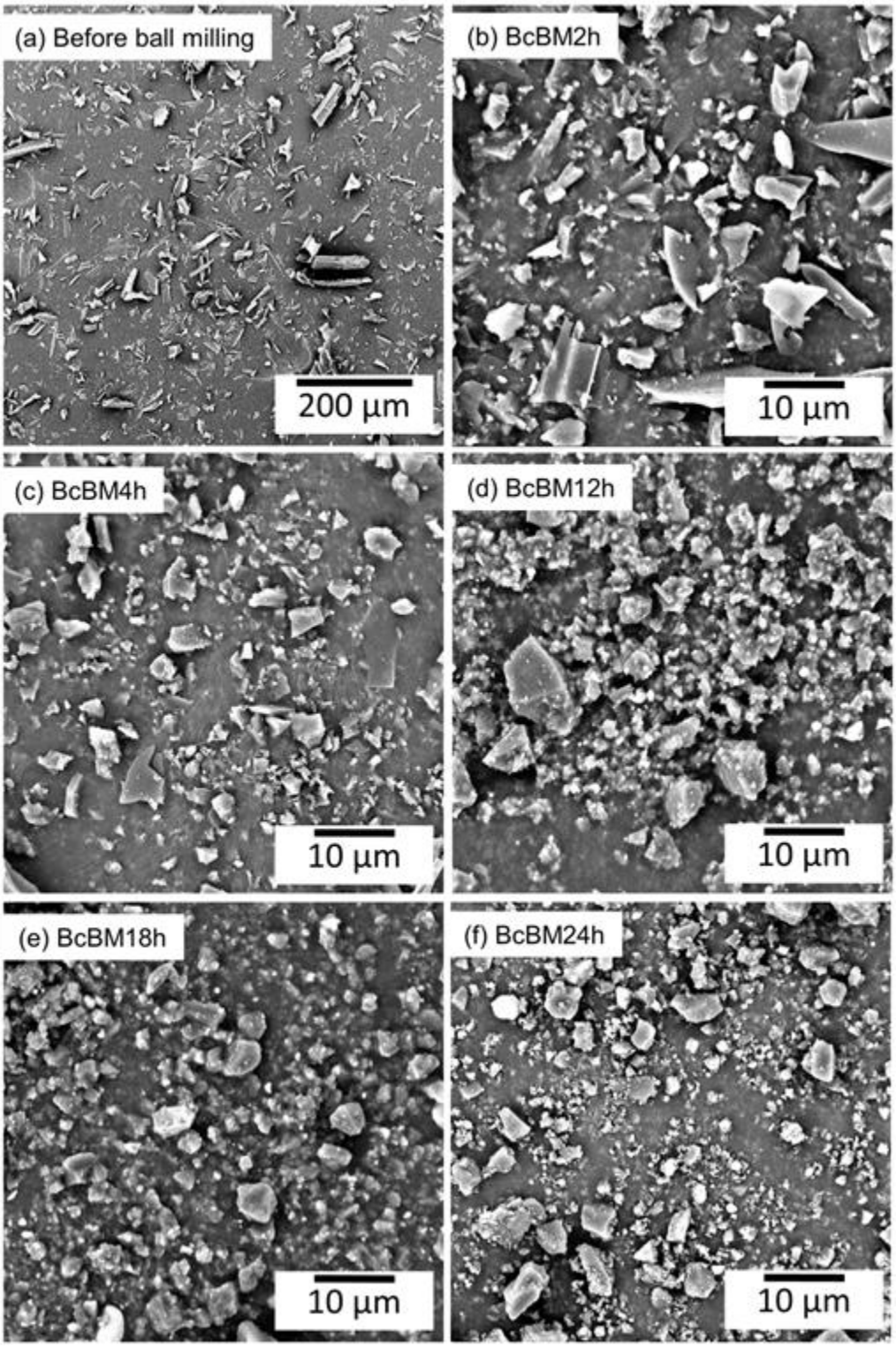

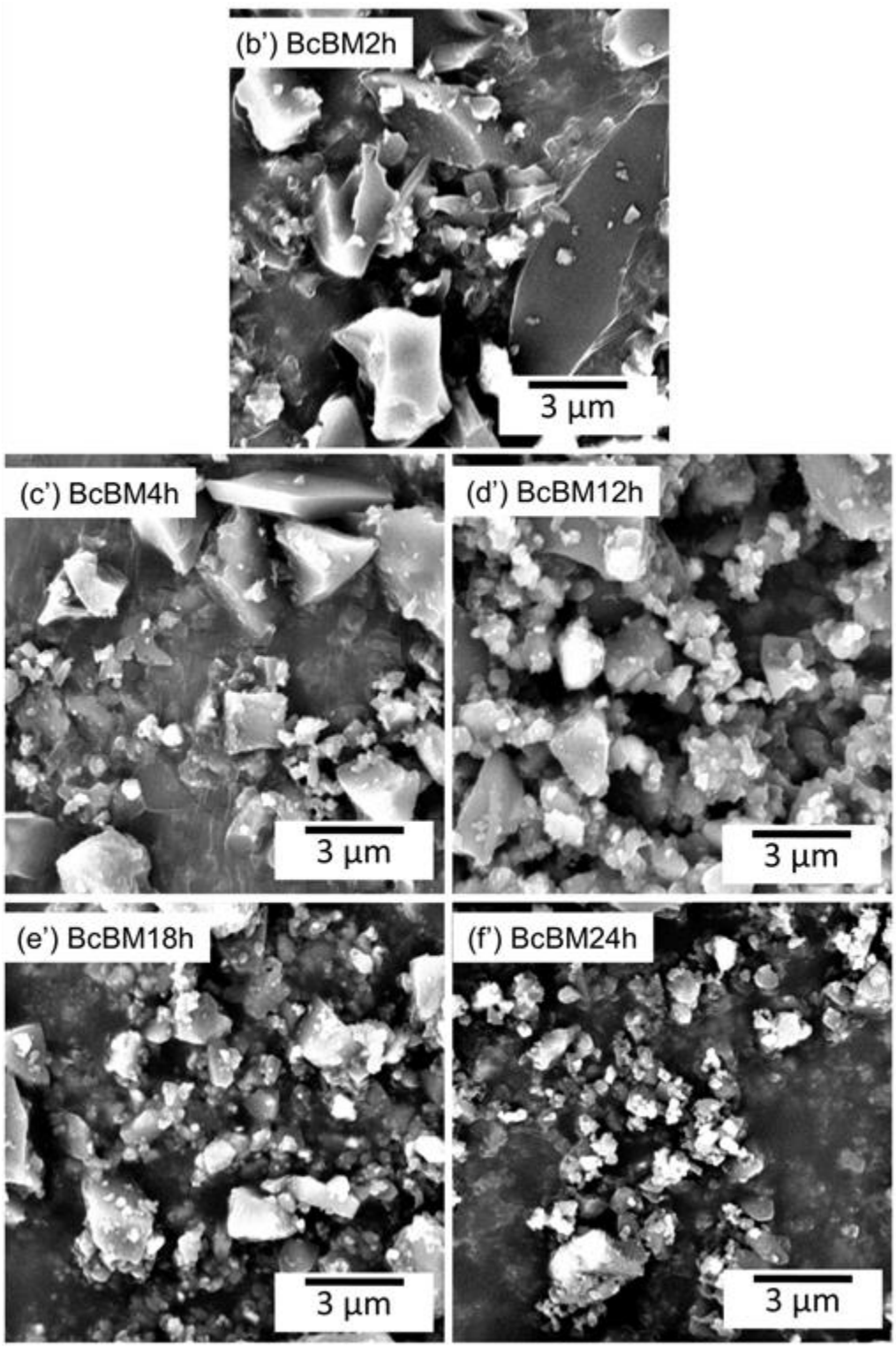

Fig. 1. SEM images of the biocarbon before and after ball milling; the samples labeled BcBM2h, BcBM4h, BcBM12h, BcBM18h, and BcBM24 were milled for 2, 4, 12, 18, and 24 h, respectively; the image in (a), the sample before ball milling, was taken at a much lower magnification than the other images

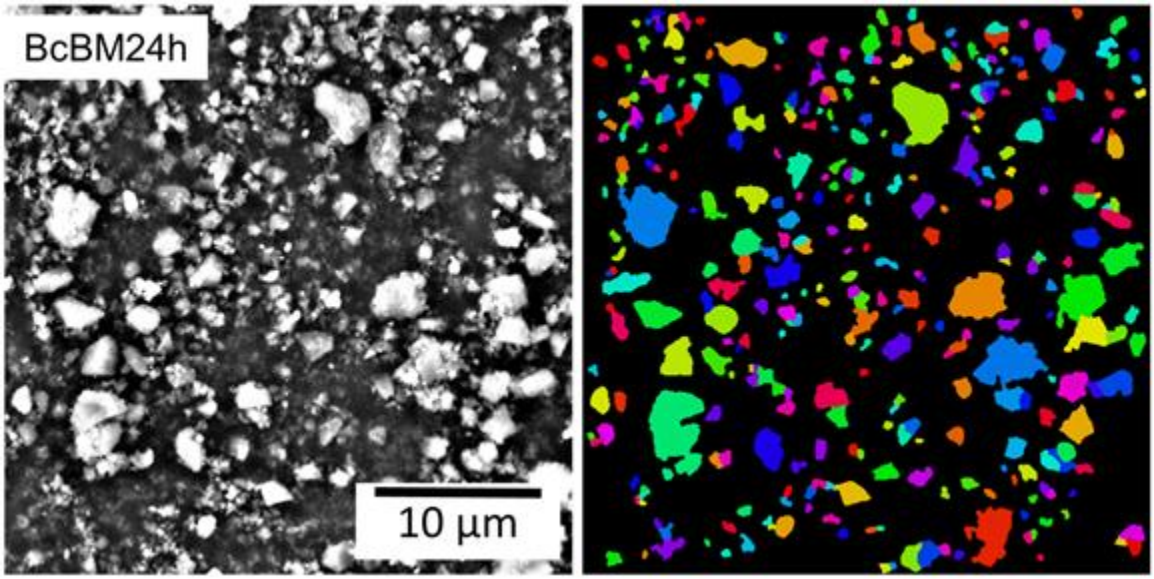

Fig. 2. SEM image of one ball-milled sample; the color picture on the right illustrates the particles recognized from the SEM image on the left; the color codes help to visually differentiate the particles and have no meaning in the measurement

The particle size distribution from the same analysis is presented in Fig. 4. The sample that was ball milled for 2 h (BcBM2h) showed the widest size distribution among all of the samples. As for the 4 h milled sample, although the highest peak shifted to a much smaller size number, the distribution was still broad.

In fact, it has been shown in Fig. 1(c) and (c') that this sample still contained plate-like pieces. Further increase of ball milling time to 12 h and 18 h clearly reduced the percentages of the large particles (Fig. 4). The 24 h milled sample showed the narrowest particle size distribution.

Minimal studies have been published on the ball milling of biocarbon. Abdullah and Wu (2009) used ball milling to grind pyrolyzed wood for 1, 2, and 4 min to enhance its properties for fuel applications. Electron microscope images showed irregular particle shape and image-based particle size analysis found that approximately 28% of the particles obtained by milling the 300 °C pyrolyzed sample for 2 min were less than 75 µm. The milling time was relatively short, and the particles obtained were still very big. In a different study, birchwood biocarbon was ground by vibratory pulverizing using a gyro puck mill (Peterson *et al.* 2016). Laser-based size analysis showed three distinctive peaks in the ranges of 100 nm to 200 nm, 0.2 µm to 1 µm, and 4 µm to 7 µm. This result corresponds to the observation made in the present work that a small number of big particles was still present even after prolonged milling. Laser-based size analysis has limitations in accurately sizing these types of materials.

In the present study, the pyrolyzed biomass retained some of the structures of the plant tissue and cell wall, which were broken down to smaller pieces during the initial stage of ball milling.

With continued milling, more and more of the bigger particles were broken apart to smaller ones, leading to a quick increase of the particle number and in turn a decrease of the number-average particle size.

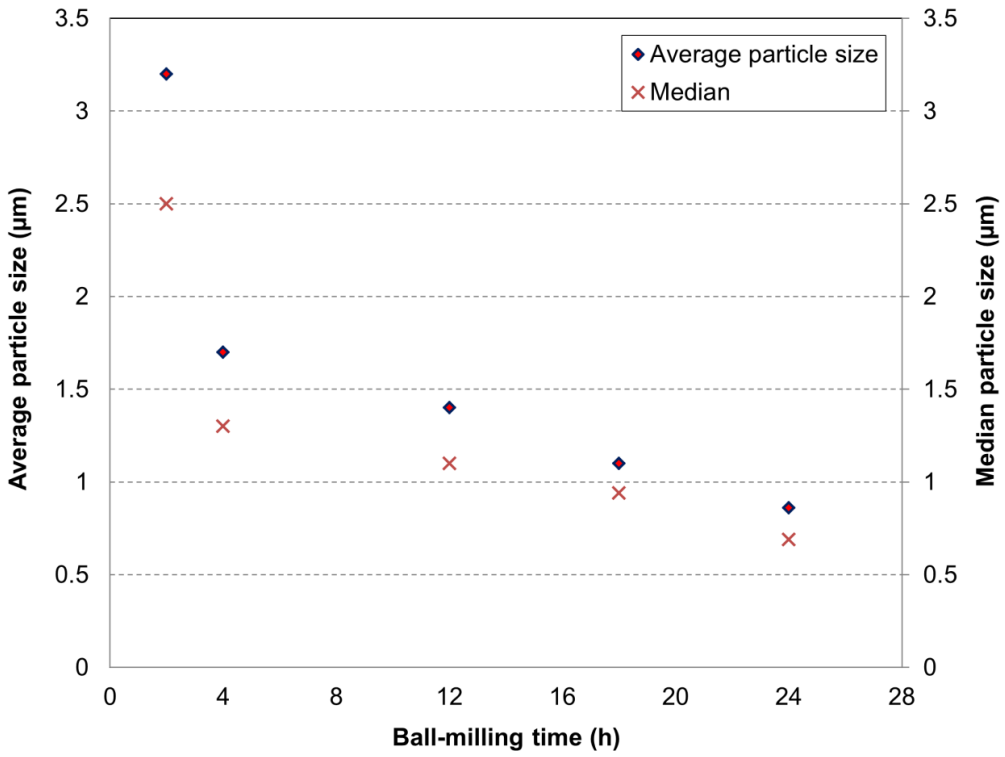

Fig. 3. Average and median particle sizes of the ball-milled biocarbon obtained by image-based size analysis

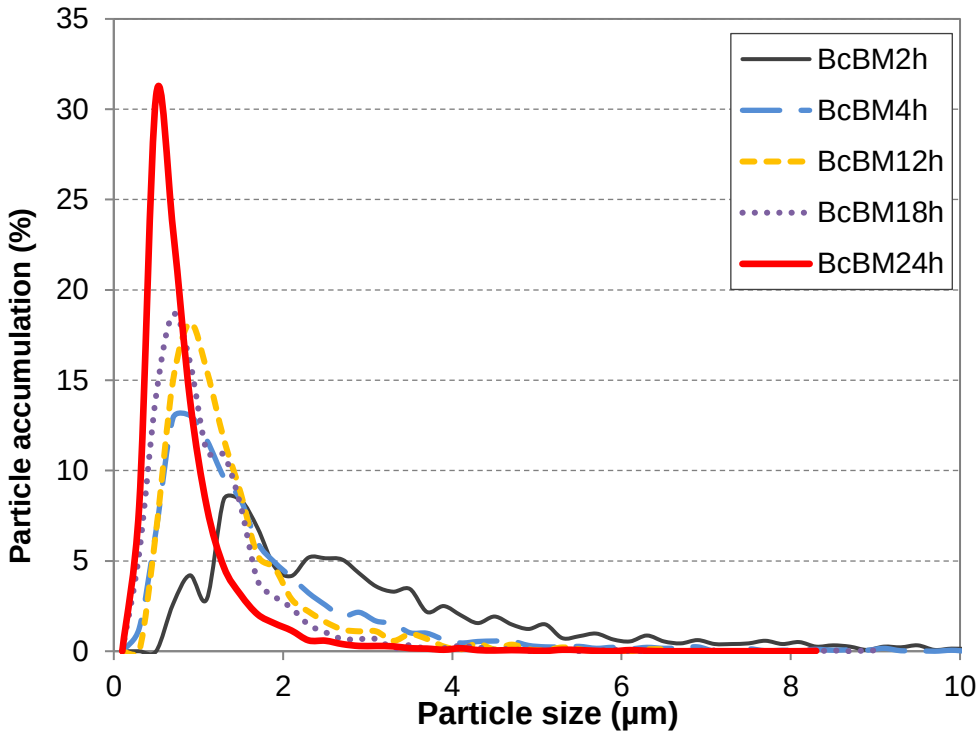

Fig. 4. Particle size distribution of the ball-milled biocarbon obtained by image-based particle size analysis (note: Although many of the samples contained particles larger than 10 μm, the percentages of those particles are very small. The portions of the curves beyond 10 μm are not shown to make the peaks on the left more visible in the figure.)

BET Surface Area

The size reduction of a material can lead to changes in its specific surface area. Figure 5 shows that the specific surface area of the sample before ball milling was 148 m^2/g and the values of the ball-milled samples were between approximately 270 m^2/g and 315 m^2/g. Longer milling time with further size reduction did not lead to greater surface area. The total pore volume had the same trend, having an initial increase and then levelling off, as shown in this same Fig. 5.

Charred biomass is known to be a porous material (Ahmad *et al.* 2014; Aller 2016). Figure 1 has shown that the initial ball milling caused considerable structural changes to the material, making more surfaces accessible. However, the fractionation of the particles with prolonged milling may have happened primarily along the large pore channels, thus causing the total surface area to remain relatively constant.

Peterson *et al.* (2012) used ball milling to increase the BET surface area of biocarbon produced from corn stover. While the unmilled material had a surface area of 3 m^2/g, the samples that were wet milled with solvents, including acetone and ethanol, for 6 h showed much higher specific surface areas, with the highest value reaching 194 m^2/g. Same as in the present work, longer milling time was found to be not helpful in further increasing the surface area. Compared to that study, the higher surface area values achieved by ball milling in the present work may have benefited from the higher surface area of the starting material (approximately 150 m^2/g). No size analysis was reported in the cited work.

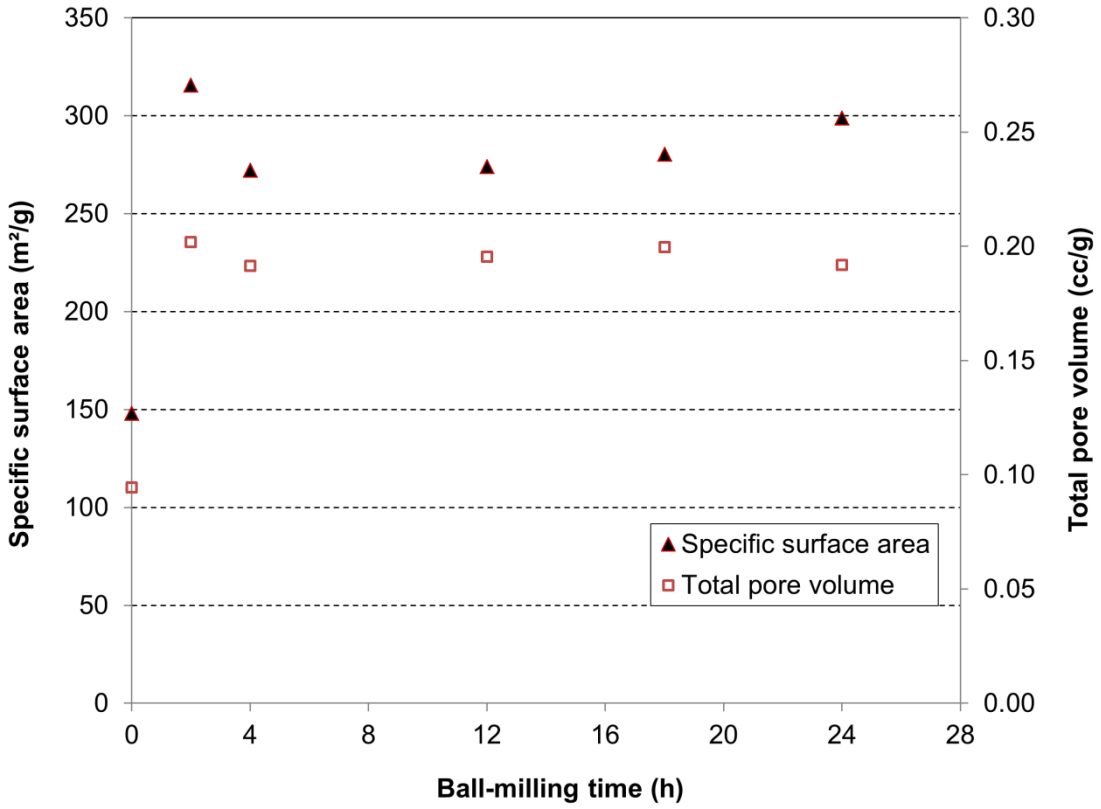

Fig. 5. Relationship between the ball-milling time and the specific surface area and total pore volume of the biocarbon

Ash Content

The ash contents of the samples were measured using a furnace at 750 °C and also TGA at 1000 °C (Table 1). The ash content increased after 2 and 4 h of milling and then leveled off at 12 and 18 h of milling. It became higher again after 24 h of milling. The ash content of the miscanthus biocarbon (before ball milling) obtained here was similar to the values of the miscanthus biocarbon (7.9%) and wood biocarbon (10.6%) reported in the literature (de la Rosa *et al.* 2014; Oginni *et al.* 2017). Moreover, the ash content of the sample before ball milling in the present work agreed well with that of the miscanthus biocarbon obtained by pyrolysis at 500 °C (8.4%), and the ash content of the sample milled for 24 h (BcBM24h) in the present work with that of the miscanthus biocarbon obtained at 900 °C (16.1%) in a previous study (Behazin *et al.* 2017). The increase of the ash content with increased pyrolysis temperature and residence time has also been reported in other literature (Ronsse *et al.* 2013; Janus *et al.* 2015). In other words, the increase of ball-milling time in the present study had the same effect on ash content changes as the increase of pyrolysis severity. Part of the high energy generated during ball milling dissipates as heat, which causes significant temperature rises. It has been found that ball milling can quickly destroy the crystalline structures of crystallized carbon to yield amorphous carbon (Li and Zhou 2010; Moshtaghioun *et al.* 2013). The process also causes the amorphous carbon to become volatile, leading to an increased concentration of inorganic components left in the samples.

Table 1. Ash Content of the Biocarbon Before and After Ball-milling

Milling Time (h)	Ash Content using Furnace at 750 °C (%)	Ash Content Using TGA at 1000 °C (%)
0	8.3 ± 0.1	8.5 ± 0.1
2	10.4 ± 0.1	11.1 ± 0.3
4	14.1 ± 0.3	14.3 ± 0.0
12	14.1 ± 0.0	14.5 ± 0.3
18	14.3 ± 0.1	14.1 ± 0.2
24	16.8 ± 0.1	17.1 ± 0.1

Thermal Conductivity and Diffusivity

The thermal conductivity and diffusivity of the samples were measured by embedding a Kapton sensor in the compacted powder. Overall, the thermal conductivity of the samples was low (Fig. 6). The conductivity decreased after 2 and 4 h of milling, stopped changing from 4 to 12 and 18 h, and then decreased again after 24 h of milling. It was interesting that this trend matched well with the ash content changes. The ash components of biocarbon obtained from grass are mostly oxides, especially silica (Brewer *et al.* 2009). The increased concentration of ash, and hence decreased carbon content, can cause a decrease in conductivity. The thermal conductivity of the biocarbon in the present work was slightly lower than that of carbon black (which has higher carbon content), usually reported to be in the range of 0.2 to 0.5 $W \cdot m^{-1} \cdot K^{-1}$ at room temperature (Khizhnyak *et al.* 1979; Snowdon *et al.* 2014).

Thermal diffusivity measures the rate of heat transfer through a material across a temperature differential. The thermal diffusivity was 0.17 $mm^2 \cdot s^{-1}$ for the biocarbon before ball milling and dropped to 0.05 $mm^2 \cdot s^{-1}$ after 2 h of ball milling. The diffusivity values remained almost the same from 2 to 24 h of milling. Because the material used for measurement was compacted powder, heat conduction through the powder mass could

have been affected by the particle-to-particle interface. The earlier observation that all of the ball-milled samples had similar relative surface area may have strong implications on their similar values of thermal diffusivity (the rate of heat transfer).

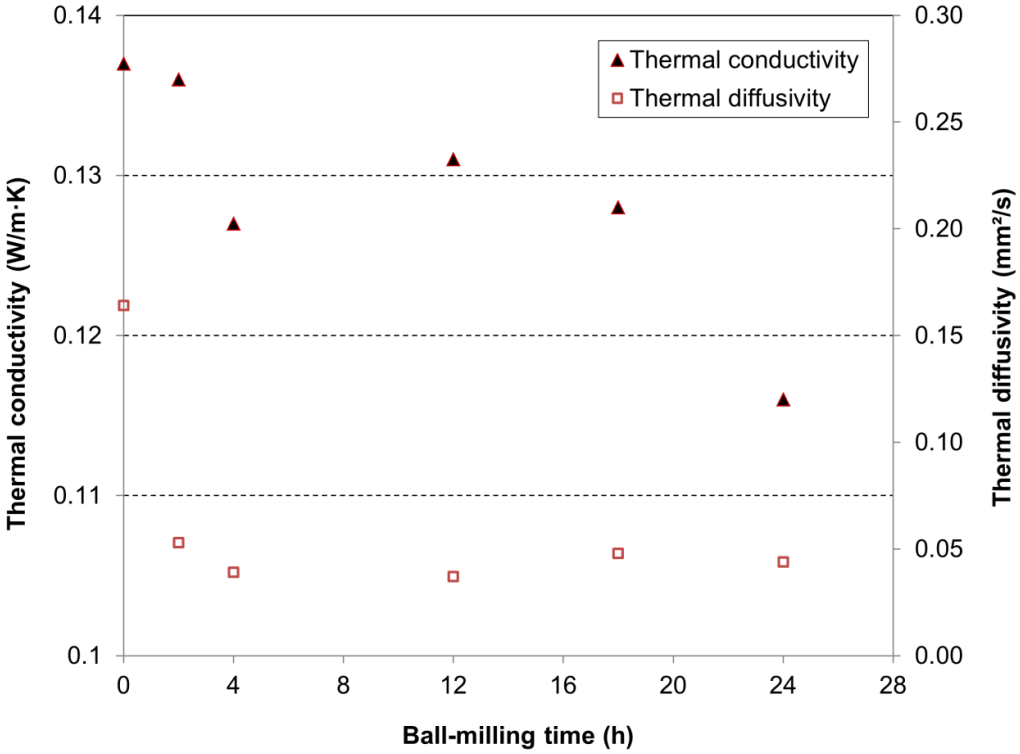

Fig. 6. Thermal conductivity and diffusivity of the biocarbon ball milled for different lengths of time

Composites Characterization – Fracture Surfaces

The practice of using fillers to improve the stiffness of plastics is common in the automotive, packaging, and other industries, with a notable example being talc reinforced polypropylene composite (Leong *et al.* 2005). A plastic car part, for example, can contain the following basic components: a polypropylene matrix, a filler such as talc, coupling agents, and other additives (Dellock *et al.* 2014; Mohanty *et al.* 2015a). While filler contents vary based on the property requirements of the final product, it is common to find filler contents between ~20 and 40% (Mohanty *et al.* 2015b; Rohrmann *et al.* 2016).

In this study, polypropylene composites filled with 27% biocarbon (before ball milling, BcBM2h, BcBM4h, and BcBM24h) were compared to the sample filled with 27% talc. The cryo-fractured surfaces of the BcBM24h composite (Fig. 7A), the composite filled with the biocarbon before ball milling (Fig. 7B), the talc composite (Fig. 7C), and the neat polypropylene (Fig. 7D) were examined by SEM imaging.

The particles found on the fracture surface of the composite filled with the biocarbon before ball milling had much inhomogeneity (Fig. 7B), showing high variation in the shape and sizes. This corresponds to the morphology of the particles observed earlier. The irregular morphology of these particles may cause inefficient stress transfer, as well as stress concentration at the sharp edges. The large particles with many defects may also fail easily under impact. The composite filled with the 24 h ball milled material showed smaller particles in the matrix and a much more homogeneous dispersion of the particles (Fig. 7A).

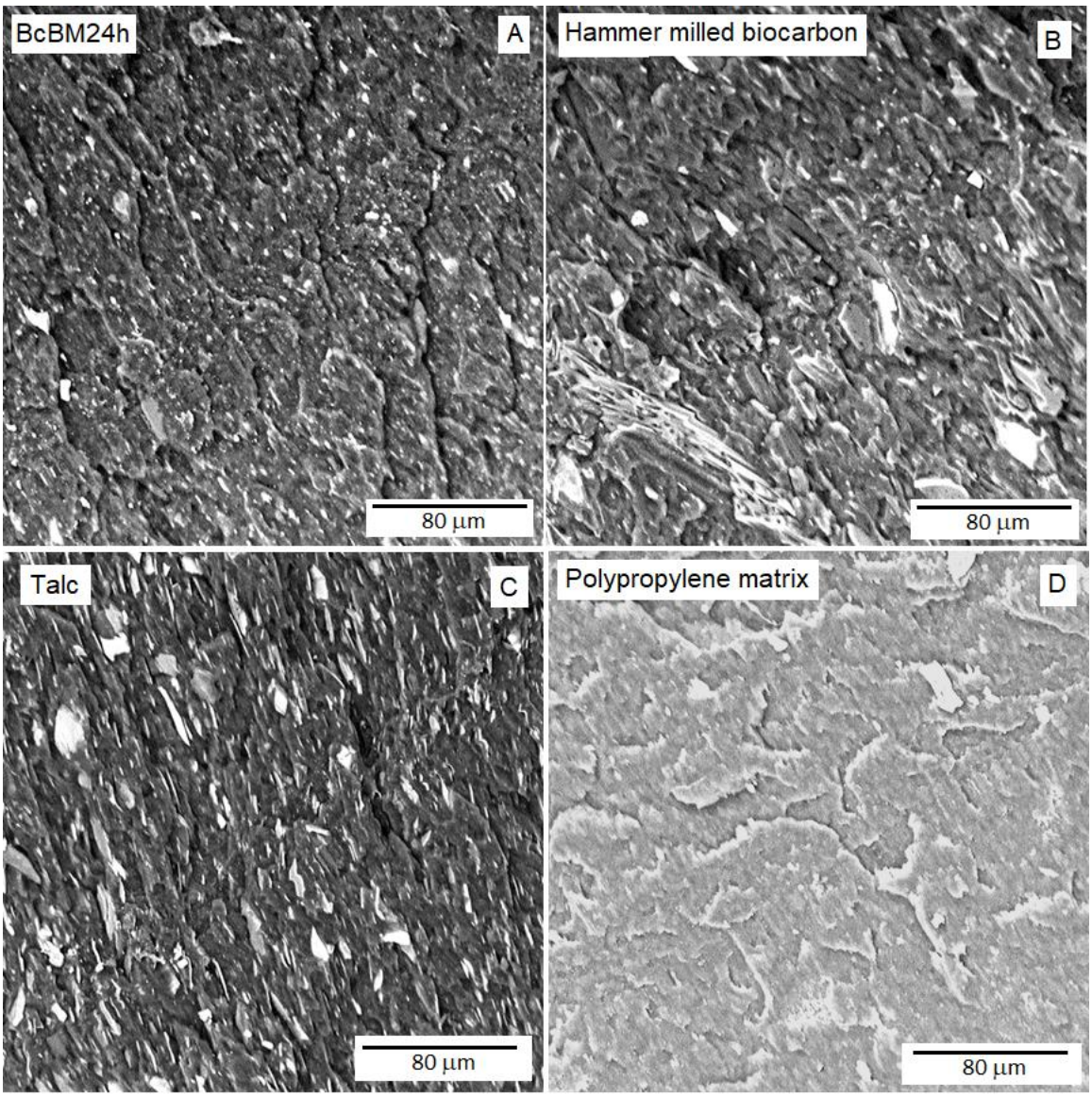

Fig. 7. SEM images of polypropylene composites filled with (A) BcBM24h; (B) biocarbon before ball milling; and (C) talc. The image in (D) is the neat polypropylene

More surface interaction can reduce the chance of particle failure under stress. Moreover, particulate fillers with smaller size and more spherical shape have been found to improve the impact strength by helping to dissipate the energy during crack propagation (Ogunsona *et al.* 2017). The talc particles found in the composite showed a platy or layered pattern (lamella) and the plates were apparently aligned in the polymer flow direction during injection molding (Fig. 7C). This pattern in talc-filled composites is a main contributor to their increased modulus (Huda *et al.* 2007).

Composites Characterization – Physical and Mechanical Properties

One of the main advantages of biocarbon is its lower density compared to mineral fillers. In this study, the density of the neat polypropylene was measured to be 0.90±0.01 g/cm^3, while the density of the 27% talc composite was 1.105±0.005 g/cm^3, a 23% increase.

In contrast, the biocarbon composites showed an average density of 1.008±0.001 g/cm^3, closer to that of polypropylene. The low density of biocarbon makes it an attractive filler material for weight reduction in product design.

One of the most important measures of quality for composite materials is their mechanical properties. Improving the specific tensile modulus of polypropylene is one of the main motivations to use fillers (Huda *et al.* 2007). Here the performance of the biocarbon in polypropylene composites is compared to that of talc, which is commonly used in the automotive industry. The specific tensile and flexural properties (based on density) are shown in Figs. 8 and 9. The specific moduli of the biocarbon composites were found to be only slightly lower than that of the talc composite (Fig. 8). There was a noted increase of the specific tensile modulus with increasing ball milling time from 2 h to 24 h, with the tensile modulus of the BcBM24 composite surpassing that of the talc composite.

In the strength comparison (Fig. 9), the talc composite and biocarbon composites had similar tensile strength, while the biocarbon composites showed higher flexural strength than the talc composite. Although there was initially a slight increase of the flexural strength with ball milling, the strength decreased with longer milling time. This gradual decrease of the flexural strength may have been caused by the milling process making the particles more spherical, hence with reduced aspect ratio.

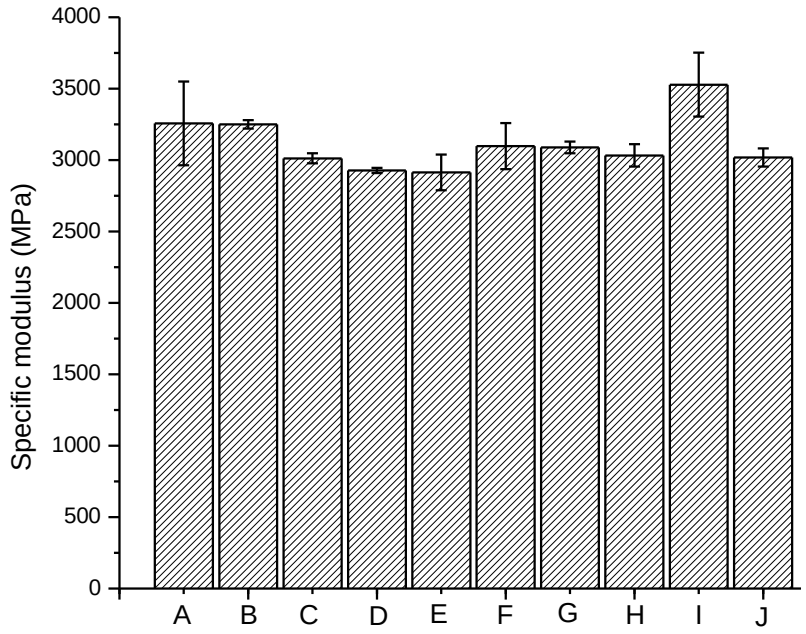

Fig. 8. Specific tensile modulus (TM) and flexural modulus (FM) of the composites filled with: (A) talc-TM; (B) talc-FM; (C) biocarbon before ball milling-TM; (D) biocarbon before ball milling-FM; (E) BcBM2h-TM; (F) BcBM2h-FM; (G) BcBM4h-TM; (H) BcBM4h-FM; (I) BcBM24h-TM; (J) BcBM24h-FM

The notched Izod and unnotched Charpy impact properties are shown in Figs. 10 and 11, respectively. The impact strength of the composite filled with the biocarbon before ball milling was only about half of that of the talc composite. However, the impact strength started to increase when the ball milled biocarbon was used and continued to rise with longer ball milling time. The impact strength of the BcBM24 composite was improved 100% from that of the composite filled with the biocarbon before ball milling and reached about the same value as that of the talc composite.

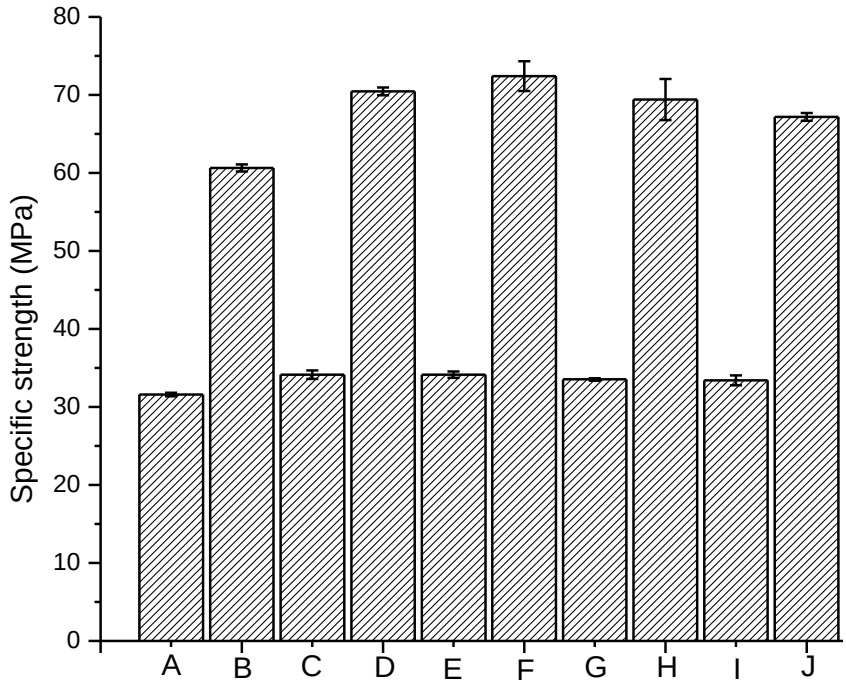

Fig. 9. Specific tensile strength (TS) and flexural strength (FS) of the composites filled with: (A) talc-TS; (B) talc-FS; (C) biocarbon before ball milling-TS; (D) biocarbon before ball milling-FS; (E) BcBM2h-TS; (F) BcBM2h-FS; (G) BcBM4h-TS; (H) BcBM4h-FS; (I) BcBM24h-TS; (J) BcBM24h-FS

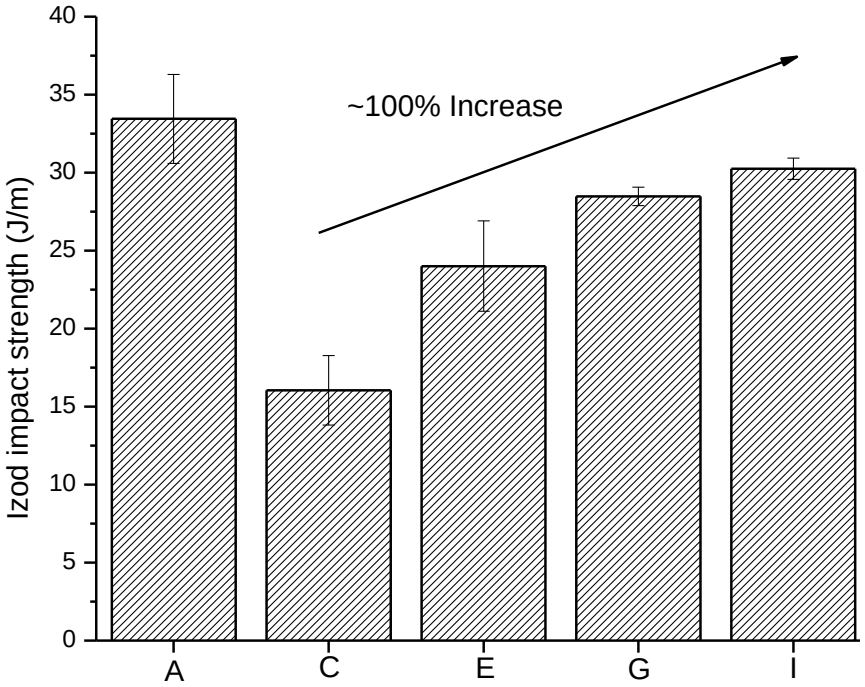

Fig. 10. Specific notched Izod impact strength of the composites filled with: (A) talc; (C) biocarbon before ball milling; (E) BcBM2h; (G) BcBM4h; (I) BcBM24h

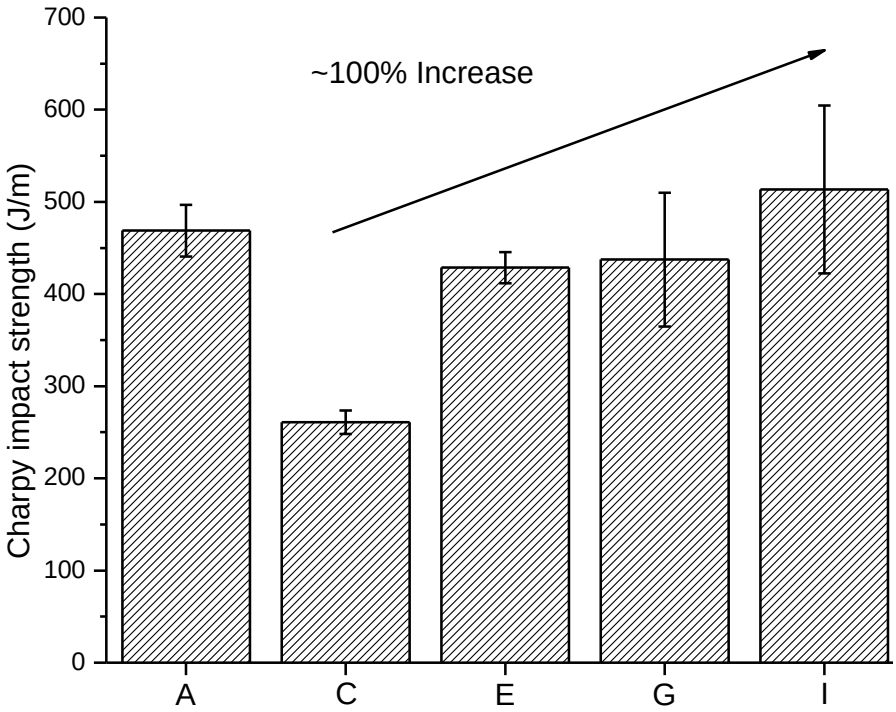

Fig. 11. Specific Charpy impact strength of the composites filled with: (A) talc; (C) biocarbon before ball milling; (E) BcBM2h; (G) BcBM4h; (I) BcBM24h

The high modulus of talc-filled composites is often attributed to the layered or platy arrangement of the talc in the matrix. The platy morphology, as shown in the SEM image in Fig. 7, is obtained by delamination during the extrusion process and plays a fundamental role in stress transfer and distribution. The size and shape changes induced to biocarbon by milling is also found to affect the properties of its composites. The addition of rigid fillers is known to interfere with the plastic deformation and reduce the toughness of polymers. The use of ball milled biocarbon with finer and more uniform particles achieved impact properties similar to that of the talc composite. The control over the particle size of the biocarbon derived from biomass can be useful for tuning the mechanical behavior and the surface quality and physical properties of the composites manufactured (Mohanty *et al.* 2015a,b).

CONCLUSIONS

1. Biocarbon obtained from miscanthus through slow pyrolysis was milled at an industry-scale ball mill facility for size reduction. SEM imaging combined with image-based particle analysis proved to be a suitable method to study the morphology changes and the evolution of the particle size and size distribution with respect to milling time.
2. The chunky pieces of the pyrolyzed material became sub-micron particles after 24 h of ball milling, and the size distribution became narrower. The specific surface area increased, from 150 m^2/g before milling to approximately 300 m^2/g after milling. However, longer milling time did not lead to further increase of the surface

area, suggesting that the rupture of the particles had most likely happened along the pores and channels of the large particles.

3. The ash content of the biocarbon increased with ball milling and doubled after 24 h of milling, which indicated the volatilization of some of the amorphous carbon during the milling process. This was accompanied by decreasing thermal conductivity of the compacted biocarbon powder with longer milling time, whereas the thermal diffusivity had an initial drop following ball milling and remained almost the same with longer milling time.
4. One of the potential applications of biocarbon with a reduced size, more uniform size distribution, and larger specific surface area is in polymer composites. The ball milled biocarbon was used to prepare polypropylene composites, which were also compared to a talc composite. The biocarbon composites had lower density than the talc composite, with comparable specific tensile and flexural properties to the latter. Particle size reduction by longer milling time was found to improve the impact resistance, with the impact strength of the BcBM24h composite reaching the same level as that of the talc composite. The biocarbon can help to meet the automotive industry's goal of reducing the weight of car parts for better fuel efficiency and increasing the usage of sustainable materials for environmental benefits.

ACKNOWLEDGMENTS

The authors are grateful for the support of Agriculture and Agri-Food Canada and Competitive Green Technologies through AgriInnovation Program (Projects No. 052882 and No. 051910); the Ontario Ministry of Agriculture, Food, and Rural Affairs - University of Guelph Bioeconomy Industrial Uses Research Program (Project No. 030055); Natural Sciences and Engineering Research Council (NSERC), Canada for the Discovery Grants Program (Project No. 401111); the NSERC Collaborative Research and Development (CRD) (Project No. 401190); the Ontario Centres of Excellence (Project No 053035); Competitive Green Technologies (Project No. 053036); and the Ontario Research Fund, Research Excellence Program Round-7 from the Ontario Ministry of Research and Innovation, currently known as the Ontario Ministry of Research, Innovation and Science (Projects No. 052665 and No. 052644).

REFERENCES CITED

Abdullah, H., and Wu, H. (2009). "Biochar as a fuel: 1. Properties and grindability of biochars produced from the pyrolysis of mallee wood under slow-heating conditions," *Energy Fuels* 23(8), 4174-4181. DOI: 10.1021/ef900494t

Ahmad, N., Rajapaksha, A. U., Lim, J. E., Zhang, M., Bolan, N., Mohan, D., Vithanage, M., Lee, S. S., and Ok, Y. S. (2014). "Biochar as a sorbent for contaminant management in soil and water: A review," *Chemosphere* 99, 19-33. DOI: 10.1016/j.chemosphere.2013.10.071

Aller, M. F. (2016). "Biochar properties: Transport, fate, and impact," *Crit. Rev. Env. Sci. Tec*. 46(14-15), 1183-1296. DOI: 10.1080/10643389.2016.1212368

Amin, F. R., Huang, Y., He, Y., Zhang, R., Liu, G., and Chen, C. (2016). "Biochar applications and modern techniques for characterization," *Clean Technol. Envir.* 18(5), 1457-1473. DOI: 10.1007/s10098-016-1218-8.

Arnold, S., Rodriguez-Uribe, A., Misra, M., and Mohanty, A. K. (2018). "Slow pyrolysis of bio-oil and studies on chemical and physical properties of the resulting new bio-carbon," *J. Clean. Prod.* 172, 2748-2758. DOI: 10.1016/j.jclepro.2017.11.137.

ASTM D256 (2010). "Standard test method for determining the Izod pendulum impact resistance of plastics," ASTM International, West Conshohocken, PA.

ASTM D638 (2014). "Standard test method for tensile properties of plastics," ASTM International, West Conshohocken, PA.

ASTM D790 (2017). "Standard test methods for flexural properties of unreinforced and reinforced plastics and electrical insulating materials," ASTM International, West Conshohocken, PA.

ASTM D1762-84 (2013). "Standard test method for chemical analysis of wood charcoal," ASTM International, West Conshohocken, PA.

ASTM D4812 (2011). "Standard test method for unnotched cantilever beam impact resistance of plastics," ASTM International, West Conshohocken, PA.

Beekman, A., Shan, D., Ali, A., Dai, W., Ward-Smith, S., and Goldenberg, M. (2005). "Micrometer-scale particle sizing by laser diffraction: Critical impact of the imaginary component of refractive index," *Pharm. Res*. 22(4), 518-522. DOI: 10.1007/s11095-005-2494-x.

Behazin, E., Ogunsona, E., Rodriguez-Uribe, A., Mohanty, A. K., Misra, M., and Anya, A. O. (2016). "Mechanical, chemical, and physical properties of wood and perennial grass biochars for possible composite application," *BioResources* 11(1), 1334-1348. DOI: 10.15376/biores.11.1.1334-1348

Behazin, E., Misra, M., and Mohanty, A. K. (2017). "Sustainable biocarbon from pyrolyzed perennial grasses and their effects on impact modified polypropylene biocomposites," *Compos. Part B-Eng.* 118, 116-124. DOI: 10.1016/j.compositesb.2017.03.003.

Blott, S. J., and Pye, K. (2006). "Particle size distribution analysis of sand-sized particles by laser diffraction: An experimental investigation of instrument sensitivity and the effects of particle shape," *Sedimentology* 53(3), 671-685. DOI: 10.1111/j.1365-3091.2006.00786.x

Brewer, C. E., Schmidt-Rohr, K., Satrio, J. A., and Brown, R. C. (2009). "Characterization of biochar from fast pyrolysis and gasification systems," *Environ. Prog. Sustain.* 28(3), 386-396. DOI: 10.1002/ep.10378

Califice, A., Michel, F., Dislaire, G., and Pirard, E. (2013). "Influence of particle shape on size distribution measurements by 3D and 2D image analyses and laser diffraction," *Powder Technol.* 237, 67-75. DOI: 10.1016/j.powtec.2013.01.003

de la Rosa, J. M., Paneque, M., Miller, A. Z., and Knicker, H. (2014). "Relating physical and chemical properties of four different biochars and their application rate to biomass production of *Lolium perenne* on a calcic cambisol during a pot experiment of 79 days," *Sci. Total Environ.* 499, 175-184. DOI: 10.1016/j.scitotenv.2014.08.025.

Dellock, P. K., Pierce, J. T., and Karmo. (2014). "Polypropylene with bio-based and synthetic fillers for light weight materials applications," US Patent 8,642,683 B1.

Huda, M. S., Drzal, L. T., Mohanty, A. K., and Misra, M. (2007). "The effect of silane treated- and untreated-talc on the mechanical and physico-mechanical properties of poly(lactic acid)/newspaper fiber/talc hybrid composites," *Compos. Part B-Eng.* 38, 367-379. DOI: 10.1016/j.compositesb.2006.06.010.

Janus, A., Pelfrêne, A., Heymans, S., Deboffe, C., Douay, F., and Waterlot, C. (2015). "Elaboration, characteristics and advantages of biochars for the management of contaminated soils with a specific overview on *Miscanthus* biochars," *J. Environ. Manage* 162, 275-289. DOI: 10.1016/j.jenvman.2015.07.056

Khizhnyak, P., Chechetkin, A., and Glybin, A. (1979). "Thermal conductivity of carbon black," *J. Eng. Phys.* 37(3), 1073-1075. DOI: 10.1007/BF00861683

Li, M., Wilkinson, D., and Patchigolla, K. (2005). "Comparison of particle size distributions measured using different techniques," *Particul. Sci. Technol.* 23(3), 265-284. DOI: 10.1080/02726350590955912

Li, Z. Q., and Zhou, Y. (2010). "Structural evolution of a graphite–diamond mixture during ball milling," *Physica B* 405(3), 1004-1010. DOI: 10.1016/j.physb.2009.10.042

Leong, Y. W., Abu Bakar, M. B., Mohd, Z. A., and Ariffin, I. A. (2005). "Effects of filler treatments on the mechanical, flow, thermal, and morphological properties of talc and calcium carbonate filled polypropylene hybrid composites," *J. Appl. Polym. Sci.* 98, 413-426. DOI: 10.1002/app.21507

Mohanty, A. K., Misra, M., Bali, A., and Rodriguez-Uribe, A. (2015a). "Renewable replacements for carbon black in composites and methods of making and using thereof," Patent WO 2015135080 A1

Mohanty, A. K., Misra, M., Rodriguez-U. A., and Vivekanandhan, V. (2015b). "Hybrid sustainable composites and methods of making and using thereof," Patent WO 2015039237

Moshtaghioun, B., Monshi, A., Abbasi, M., and Karimzadeh, F. (2013). "The effect of crystallinity of carbon source on mechanically activated carbothermic synthesis of nano-sized SiC powders," *J. Mater. Eng. Perform.* 22(2), 421-426. DOI: 10.1007/s11665-012-0296-y

Naito, M., Hayakawa, O., Nakahira, K., Mori, H., and Tsubaki, J. (1998). "Effect of particle shape on the particle size distribution measured with commercial equipment," *Powder Technol*. 100(1), 52-60. DOI: 10.1016/S0032-5910(98)00052-7

Oginni, O., Singh, K., and Zondlo, J. W. (2017). "Pyrolysis of dedicated bioenergy crops grown on reclaimed mine land in West Virginia," *J. Anal. Appl. Pyrol.* 123, 319-329. DOI: 10.1016/j.jaap.2016.11.013.

Ogunsona, E., Misra, M., and Mohanty, A. K. (2017). "Sustainable biocomposites from biobased polyamide 6, 10 and biocarbon from pyrolyzed miscanthus fibers," *J. Appl. Polym. Sci.* 134(4), 44221. DOI:10.1002/app.44221,

Peterson, S. C. (2012). "Evaluating corn starch and corn stover biochar as renewable filler in carboxylated styrene-butadiene rubber composites," *J. Elastom. Plast.* 44(1), 43-54. DOI: 10.1177/0095244311414011.

Peterson, S. C., Chandrasekaran, S. R., and Sharma, B. K. (2016). "Birchwood biochar as partial carbon black replacement in styrene-butadiene rubber composites," *J. Elastom. Plast.* 48(4), 305-316. DOI: 10.1177/0095244315576241.

Peterson, S. C., Jackson, M. A., Kim, S., and Palmquist, D. E. (2012). "Increasing biochar surface area: Optimization of ball milling parameters," *Powder Technol.* 228, 115-120. DOI: 10.1016/j.powtec.2012.05.005.

Rohrmann, J., Licht, E. H., and Ahrenberg, B. (2016). "Mineral filled polypropylene composition," US Patent 0024287 A1.

Ronsse, F., Van Hecke, S., Dickinson, D., and Prins, W. (2013). "Production and characterization of slow pyrolysis biochar: Influence of feedstock type and pyrolysis conditions," *GCB Bioenergy* 5(2), 104-115. DOI: 10.1111/gcbb.12018

Snowdon, M. R., Mohanty, A. K., and Misra, M. (2014). "A study of carbonized lignin as an alternative to carbon black," *ACS Sustain. Chem. Eng.* 2(5), 1257-1263. DOI: 10.1021/sc500086v.

Article submitted: October 11, 2017; Peer review completed: January 6, 2018; Revised version received: March 14, 2018; Further revisions received and accepted: March 24, 2018; Published: April 2, 2018.
DOI: 10.15376/biores.13.2.3720-3739